

Silicone Joint Dimensioning Calculation Methods

Pierre Descamps, Valérie Hayez

Dow Silicones Belgium, Belgium, valerie.hayez@dow.com

Historically, silicone joint dimensioning is calculated with a simplified equation implemented in various standards for structural glazing. This equation assumes homogeneous stress distribution along the sealant bite whilst high local stress peaks, structure deformation or material ageing are included in a global safety factor. Safeguards such as a maximum authorized deflection (1%) and aspect ratio to respect (between 1 and 3) have been given to ensure the validity of the used equations. However new trends in commercial buildings such as the use of large dimensions glass panes or stronger engineering performance requirements such as high windloads above 5000Pa lead to the non-respect of these guidelines and the impossibility to use the simplified equation. An improved mathematical relationship making a direct correspondence between a joint included in a façade system and the behavior of a test piece was recently proposed by the authors. The goal of this article is to further validate the proposed relationship by confronting predictions with physical measurements on various test samples and the results from FEA modeling. The domain of validity of the simplified equation and the improved equation will be developed.

Keywords: silicone, joint dimensioning, calculation, modeling

1. Introduction

Bonding of glass onto aluminum frames, known as Structural Silicone Glazing (SSG), has been applied for more than 50 years on facades. Traditionally, the silicone bite is calculated using a simplified equation assuming a homogenous stress distribution along the sealant bite (ETAG 2012). Due to the complexity of façade designs (such as for example large glass dimensions or high windloads) the assumptions of limited glass deflection (maximum 1%) and aspect ratio (between 1 and 3) ensuring the validity of the simplified equations are sometimes not respected. For those projects leading to heterogeneous stress distribution in the joint, where the ETAG approach cannot be followed, Finite Element Analysis (FEA) is a popular yet expensive and complex solution since there is no standardized methodology to run FEA for evaluation of SSG.

Hence, a next generation calculation method was developed and proposed in (Descamps 2017) to replace ETAG equation when its safeguards cannot be respected. The new calculation method models the silicone joint using a spring. However silicones are incompressible whilst springs do not give the possibility to take into account material volume conservation. On the other hand, (Feynman 1963) demonstrated that incompressibility can be taken into account by replacing the Young modulus by a rigidity modulus which was done for the springs modelling the joints.

$$P_{wind} \frac{a}{2} = 2C_{10} \left\{ \left(1 + \frac{\Delta e}{e} \right) W + \frac{tg(\alpha)}{2e} W^2 + \frac{1}{\frac{tg(\alpha)}{e} \left(\frac{1}{1 + \frac{\Delta e}{e} + \frac{tg(\alpha)}{e} W} - \frac{1}{1 + \frac{\Delta e}{e}} \right)} \right\} \quad (1)$$

With a = small plate dimension, P_{wind} = windload, Δe =joint strain, e = joint thickness, α = angle of rotation, w = bite.

The proposed improved equation 1 incorporates a series of parameters whose values must be either measured or calculated (FEA modelling) with good accuracy as they have a large impact on the joint deformation and consequently on the conclusions drawn about joint long term durability.

The law linking the rigidity factor to the joint aspect ratio is critical; we must confirm that, as derived by FEA modeling (Descamps 2017), the rigidity factor measured experimentally is only dependent on the joint aspect ratio and not on the absolute joint dimensions.

The tensile strength and strain as a function of joint aspect ratio must be measured. It is likely that a joint of large aspect ratio possesses a lower capability to sustain an imposed deformation and so should have a lower strain at break but this has to be demonstrated experimentally. If this is the case, the mathematical relation linking the strain to the joint aspect ratio should also be derived.

The rotation angle α of the joint must also be calculated with a good accuracy as the maximum deformation imposed to the structural joint is highly dependent on α . To carry-out this calculation, the deflection of a glass pane must be calculated taking into account the geometric non-linearities. We will show that even for a glass pane deflection of 1% as allowed in ETAG, the Kirchhoff-Love approximated linear solution introduces a significant error in overestimating

the glass pane deflection. Furthermore, the glass pane deflection is influenced not only by the presence of a joint (we deviate from the simply supported assumption) but also by the joint rigidity which depends on its geometry. We have shown (Descamps 2017) that increasing the joint aspect ratio increases joint rigidity in traction and changes the joint contribution to the reduction of the glass pane deflection. This effect was illustrated but without proposing an approximate method to introduce this effect into a simplified model.

2. Experimental validation

This paragraph describes the validation of the previously described aspects (rigidity factor, tensile strength and strain as a function of aspect ratio) by calculation of the engineering strain (or equivalently, the engineering stress) for the façade joint and comparison with the stress-strain behavior measured experimentally on an H-bar sample having the same aspect ratio. Compared to (Descamps 2017), the experimental testing was extended to include more aspect ratios covering a larger range of joint dimensions. The modeling was done using 3D instead of 2D Finite Element Analysis, paying specific attention to refine the material parameters, using an optimized meshing scenario and determining the best parameter for material evaluation. Several polynomial laws linking the strain, tensile strength and rigidity factors with the aspect ratio were derived from both the experimental data and the modeling to compare the accuracy of the used model.

2.1. Methodology

A series of H-pieces with varying dimensions and aspect ratios AR (bite w/thickness e) were manufactured for experimental testing. All dimensions were chosen to be at least 8mm. From a production point of view, the injection of the product in a space smaller than this can be difficult. Hence, smaller dimensions could lead to a relatively important difference and error between the required dimension and the cured dimension. From another side, we also respected as much as possible that one joint dimension (length of 50mm) would dominate the other two dimensions. Therefore, the following H-pieces were produced:

Table 1: dimensions of studied H-pieces (in mm) and corresponding aspect ratio (Bite w/Thickness e).

Specimen	Dimensions Bite x Thickness [mm]	Aspect ratio AR
1	8 x 16	0.5
2	12 x 24	0.5
3	9 x 9	1
4	12 x 12	1
5	12 x 8	1.5
6	21 x 14	1.5
7	30 x 15	2
8	16 x 8	2
9	20 x 8	2.5
10	30 x 12	2.5
11	24 x 8	3
12	36 x 12	3

PTFE spacers with a length of 50mm, a thickness of 12mm and a third dimension of 8, 9, 12, 14, 15, 16 or 24mm were used to ensure correct joint dimensions and avoid potential influence of Norton tape as experienced in (Descamps 2017). Dowsil® 993 was used in a 10:1 mixing ratio. The H pieces were left for curing during 2 weeks before performing tensile tests to rupture.

2.2. Tensile strength dependence on Aspect Ratio and law identification

The below graphs show the Stress (MPa) versus strain (%) for the different H-piece dimensions and aspect ratios.

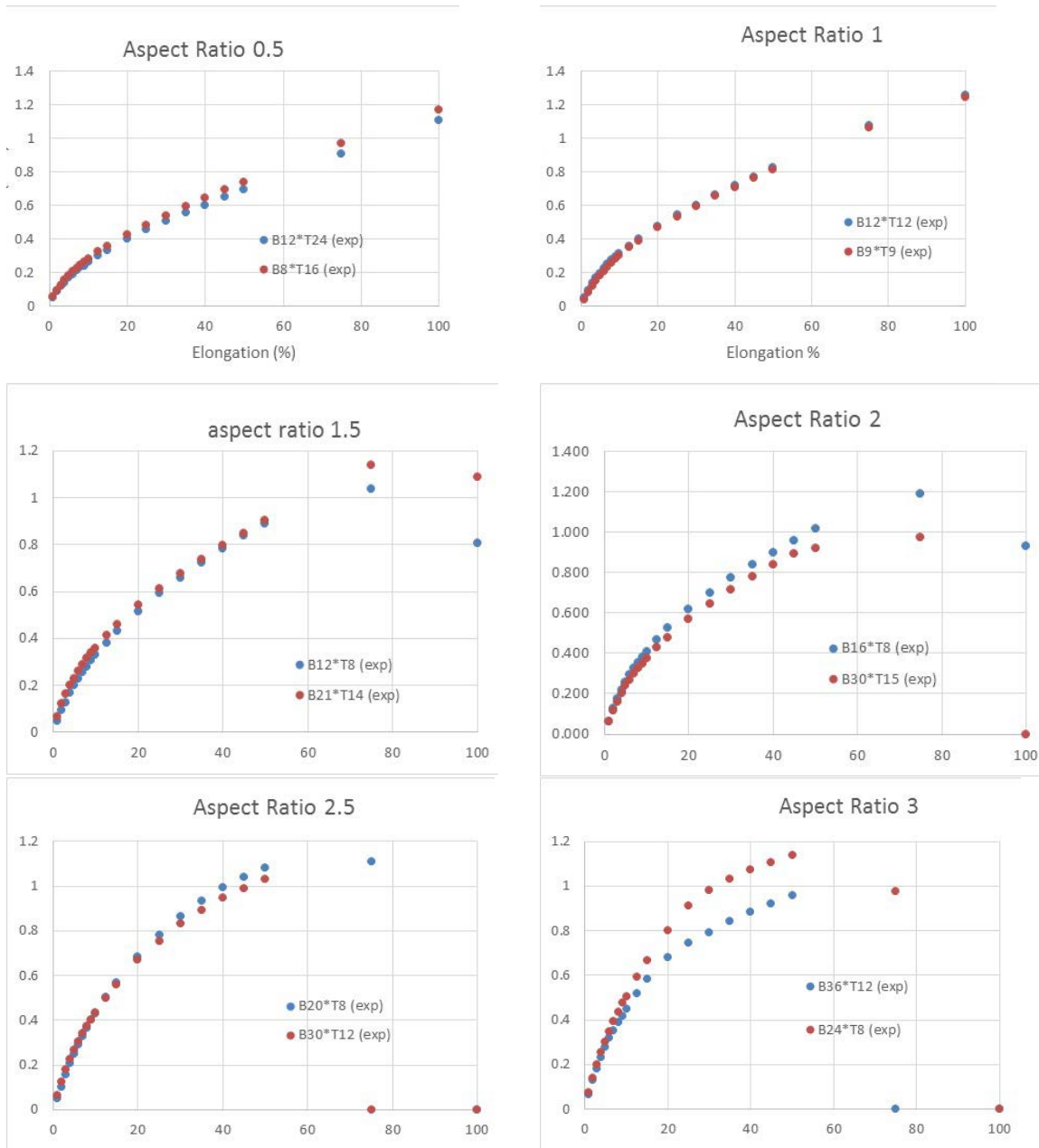


Fig. 1: Stress (MPa) versus strain (%) for the different aspect ratios and H-piece dimensions

We observe a good correspondence between the behaviors of 2 samples with the same aspect ratio. As the aspect ratio increases, we observe a gradual increase of stress for a same strain (at 20%, the stress increases from 0.4MPa for AR=0.5 to 0.7MPa for AR=3). The stress at rupture is almost constant around 1-1.2MPa independent of the AR.

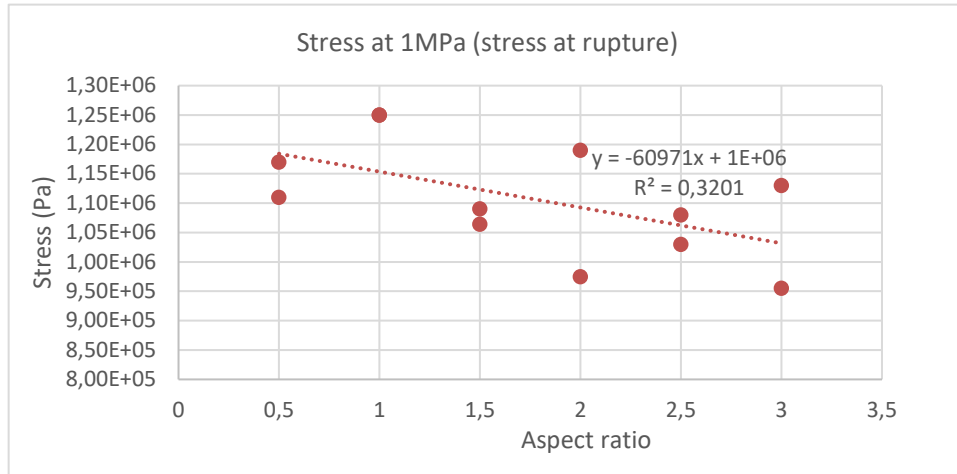


Fig. 2: Stress (MPa) versus Aspect ratio for the different H-pieces

A polynomial (linear) law linking the stress at rupture and the aspect ratio is derived from the above data-points

$$\text{Stress} = -60971 \text{ AR} + (1\text{E}+06) \quad (2)$$

2.3. Strain dependence on Aspect Ratio and law derivation

As seen on Figure 1 the maximum strain at failure decreases with increasing aspect ratio. To obtain the polynomial law linking strain and aspect ratio, we plot the strain at 1MPa (failure) versus AR on Figure 3.

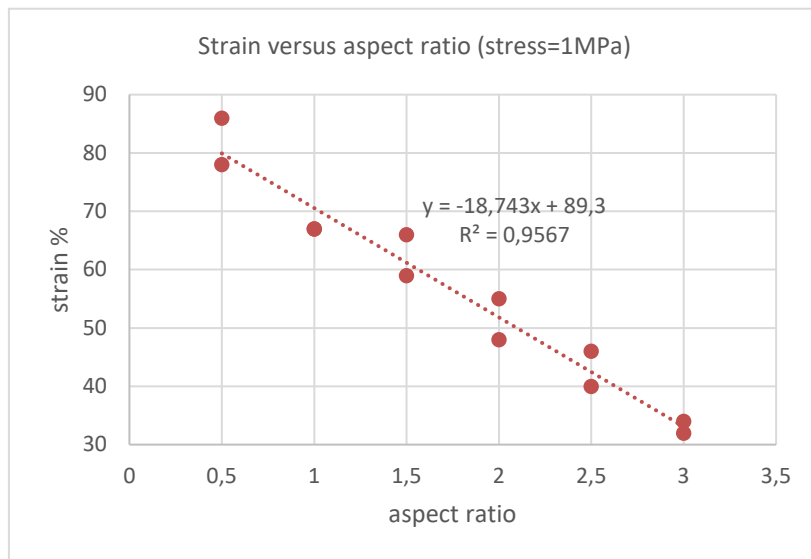


Fig. 3: Strain (%) versus Aspect ratio for the different H-pieces and derived polynomial law

A linear relationship is obtained between strain and aspect ratio

$$\epsilon (\%) = -18.743 \text{ AR} + 89.3 \quad (3)$$

Whereas the well-known 12x12x50mm³ H-piece (aspect ratio=1) reaches about 70% strain at 1MPa stress, an H-piece of 24x8x50mm³ (AR=3) will only have reached about 30% strain at the same stress. This confirms that although the stress at rupture will be very similar for all H-pieces, independent of their geometry, their strain at rupture will be much different. This corresponds with the predicted effect of rigidification occurring with increasing aspect ratio.

2.4. Rigidity factor dependence on aspect ratio and law derivation

The effective or rigidity modulus (dependent on H piece aspect ratio) is obtained by multiplying the Young modulus (material property, independent of the geometry) with the rigidity factor f_{rigidity} (Descamps 2017):

$$f_{rigidity} * E_{Young} = E_{rigidity} \quad (4)$$

Similar to the previous equation, the shear modulus G is multiplied by the rigidity factor to take into account the effect of the joint aspect ratio:

$$\sigma = f_{rigidity} G \left(1 + \varepsilon - \frac{1}{(1 + \varepsilon)^2} \right) \quad (5)$$

The measured stress-strain data were used to derive manually and sequentially the rigidity factor by fitting the above Neo-Hookean relationship. A rigidity factor is chosen arbitrarily and the corresponding stress using the Neo-Hookean relationship is calculated up to 15% strain. Only the lower part of the strain is fitted to avoid, for certain geometries, to be in the zone of material failure since this physics (material failure model) is not included in the model. The squared differences χ^2 between the measured stress and the fitted stress are calculated. The sum of the χ^2 is minimized by adapting sequentially the initial rigidity factor. This process was repeated for each of the measured H-pieces. The identified rigidity factors for each H-piece were consequently plotted as a function of the aspect ratio of the H-piece, with the intercept being set to one for the dog-bone test piece (aspect ratio 0 and rigidity factor 1) because in this case the actual modulus is equal to the Young modulus. The relationship between the rigidity factor and the aspect ratio is linear

$$f_{rigidity} = 0.5743 AR + 1.52 \quad (6)$$

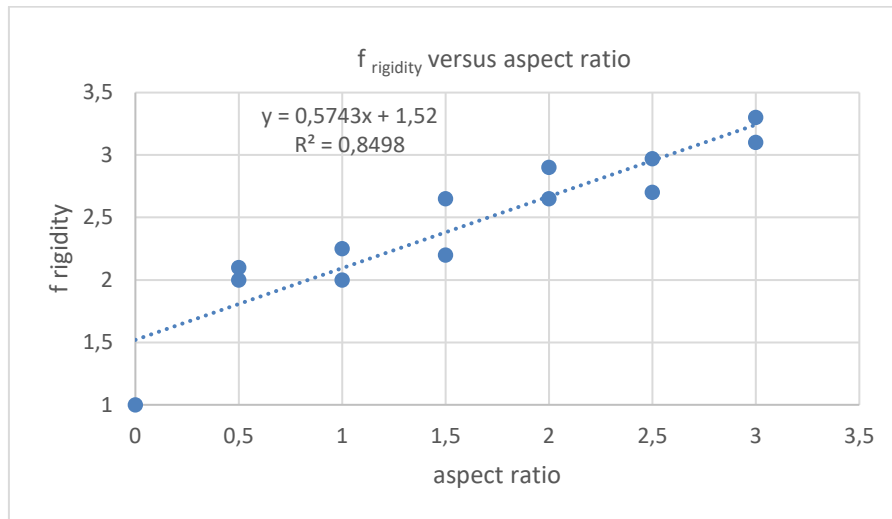


Fig. 4: rigidity factor as a function of aspect ratio using all the measured H pieces

3. Validation through 3D FEA

3.1. Method

(Descamps 2017) describes how the material properties were obtained through uniaxial, equal biaxial and pure compression testing for Dowsil 993 at Axel laboratories (Axel 2018).

The following assumptions were taken in COMSOL (Comsol 2018) for Dowsil 993. The material is assumed to be nearly incompressible whereby energy of deformation and of volume variation are separated to avoid locking. We use a Neo-Hookean model to describe the material behavior. Parameter values are listed in Table 2.

Table 2: Parameters defining silicone and glass.

parameter	value
Density 993	$\rho = 1100 \text{ kg/m}^3$
Poisson coefficient 993	$\nu = 0.49$
Young modulus 993	$E = 1.95 \text{ MPa}$
Shear Modulus 993	$G = \frac{E}{2(1+\nu)}$
Compression (isostatic) modulus 993	$K = \frac{E}{3(1-2\nu)}$
Young modulus glass	$E = 7.2 \cdot 10^{10} \text{ Pa}$
Poisson coefficient glass	$\nu = 0.27$

3.2. FEA validation of the experimental polynomial laws of stress, strain and rigidity factor versus aspect ratios

Similar to what was done above experimentally, we determined the polynomial laws between the stress, strain and rigidity factor and the aspect ratio through 3D FEA. We obtain a very good correspondence between the experimental and modelled laws. As an illustration, the experimental and modelled laws for the strain versus aspect ratio are plotted on the next figure. For all the future calculations only the experimentally derived relationships will be used.

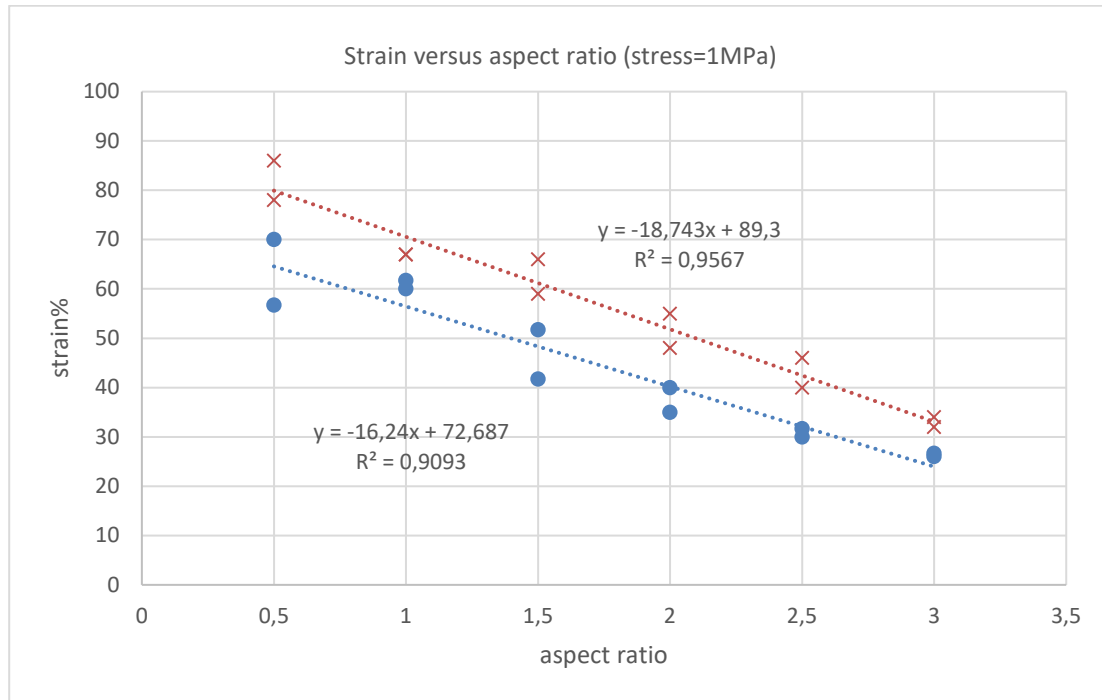


Fig. 5: strain versus aspect ratio (at stress= 1MPa) for both experimental (■) and modelled data (●)

The validity of the deduced relationships was proven experimentally for the aspect ratios 0.5-3. In this domain, the relationship between rigidity factor and aspect ratio follows a linear law. It is however not recommended to extrapolate the relationship and use it outside its domain of validity, i.e. $0 < \text{aspect ratio} < 3$ without experimental validation.

4. Deflection study

4.1. Calculating the deflection of a simply supported glass plate

When considering deflections lower or equal to 1%, both the angle of rotation of the glass at its edge and joint lateral displacement are small, hence it is believed that the joint itself should have a small impact on the plate deformation. Therefore, as a first approximation in the previously derived joint dimensioning formula (equation 1), the angle of rotation was calculated assuming a simply supported glass plate.

In the next paragraphs, we will first explain that when calculating the bending of a simply supported plate, it is critical to consider the tension forces in the middle plane of the plate, those forces being associated to the bending of the plate. Then, we will propose an approximate method to include the contribution of the joint limiting the plate deflection at its center.

Deflection of a simply supported glass plate

When calculating the deflection of a simply supported glass plate, the system of non-linear equations proposed by Foppl - Von Karman (VK) takes into account the tension forces acting in the middle plane of the plate and allows an accurate calculation of large deflections of an isotropic simply supported plate experiencing a load.

When the plate deflection becomes small compared to plate thickness, those tension forces due to plate bending can be neglected and the plate bending is calculated solving the equation proposed by Kirchhoff-Love (KL). The solution of KL equation shows a linear dependence of the plate deflection at its center on the value of the homogenously distributed load applying to the plate:

$$\frac{D \pi^6}{16 b^4} (1 + \lambda^2)^2 \omega_{1,1} = q \tag{7}$$

With λ = plate aspect ratio b/a , D = flexural rigidity of the isotropic plate, $\omega_{1,1}$ = the amplitude of the plate deflection associated to the fundamental mode and q = load

Because of its simplicity, this equation is very often used in technical guides, while its domain of validity is rather narrow. It is important to verify if the range of parameters often specified in structurally glazed facades are within the domain of validity of KL solution and hence make it a suitable equation for treating SSG projects or if a more accurate solution of the VK equations must be used.

A solution of the VK equation for a simply supported plate under a transversal load has been proposed by (Chia 1995) whereby it is assumed that the stress q is homogenously distributed over the plate surface. The plate deformation is modelled by a shape function satisfying the boundary conditions of zero deflection at $x=0$, $x=a$, $y=0$, $y=b$:

$$\omega(x, y) = \sum_{m,n} \omega_{m,n} \sin\left(\frac{n \pi x}{a}\right) \sin\left(\frac{m \pi y}{b}\right) \tag{8}$$

With ω = glass pane deflection and ω_{nm} = amplitude of the m,n deflection mode.

As a first approximation, we will limit in equation 8 the plate deflection law to the first term of a Fourier series:

$$\omega(x, y) = \omega_{1,1} \sin\left(\frac{\pi x}{a}\right) \sin\left(\frac{\pi y}{b}\right) \tag{9}$$

The simplified Chia solution to VK corresponding to the maximum plate deflection at its center is:

$$\frac{D \pi^6}{16 b^4} (1 + \lambda^2)^2 \omega_{1,1} - \frac{E h \pi^6}{8 a^2 b^2} (d_{01} + d_{10}) \omega_{1,1}^3 = q \tag{10}$$

With E = glass Young's modulus, h = glass plate thickness and d_{01} and d_{10} are the Fourier coefficient of the Airy stress function.

When the second term of equation (10) is set to zero (the term in $\omega_{1,1}^3$ can be neglected for small deflections), we retrieve the plate deflection formula calculated resolving the KL equation i.e. the deflection of the plate is proportional to the applied load q .

In the next paragraph both solutions to VK, the KL simplification and the Chia solution are studied to determine their usability for our calculations.

The glass pate deflection as a function of external load q is calculated resolving the third order equation 10 and the results are compared to the results of FEA calculations.

FEA calculations were done simulating the glass plate by a shell, having geometric non-linearities being included in the model (i.e. not using KL assumption). The advantage of using shells instead of solid elements is to increase the calculation and convergence speed by reducing the number of nodes, moving to a 2D problem. It also provides more

accuracy for the study of a glass plate which is thin in comparison with its dimensions and its deformation. The range of values explored are summarized in table 3.

Table 3: Parameters varied for the comparison of the approximated solution of Von Karman equation and the plate deflection calculated by FEA.

a	Aspect ratio	h	q
1	1	6	5000 and 10000
	2		
	3		
	4		
	5		
1	2	10	5000
	4		
	5		
2	1	6	5000
	2		
	2.5		
2	1	14	10000
	2		
	3		

On figure 6, we compare the result of glass pate deflection calculated using the approximated solution of Chia (equation 10) to the FEA results.

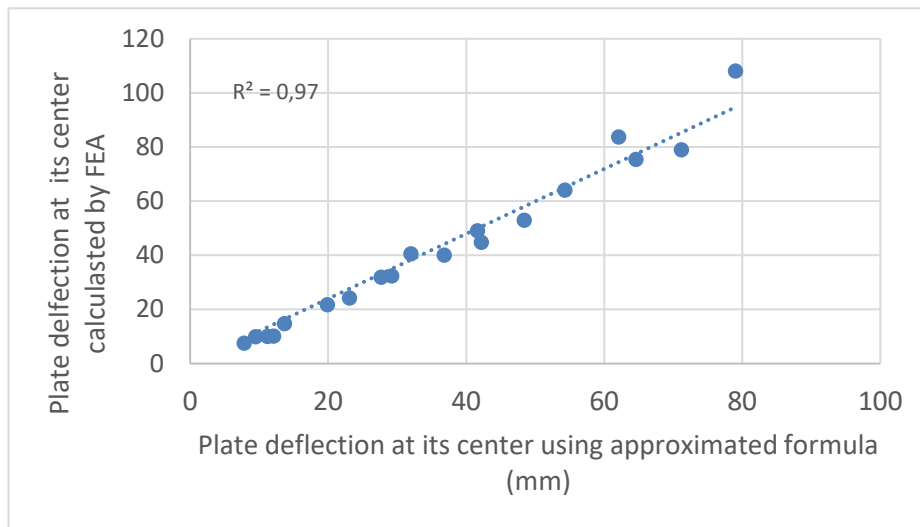


Fig. 6: Comparison between the maximum values of plate deflection at its center calculated using the approximated solution proposed by Chia and results obtained by FEA modelling

We observe a good agreement between the simplified relationship of the approximated solution and the FEA results, justifying the assumption to consider only the first term of Fourier development.

On figure 7, we plot the glass plate deflection at its center calculated using the Chia solution (equation 10) and the KL approximation (equation 7) as a function of the transversal load q. We assume the plate dimensions a, b = 1m and the glass thickness h = 6mm.

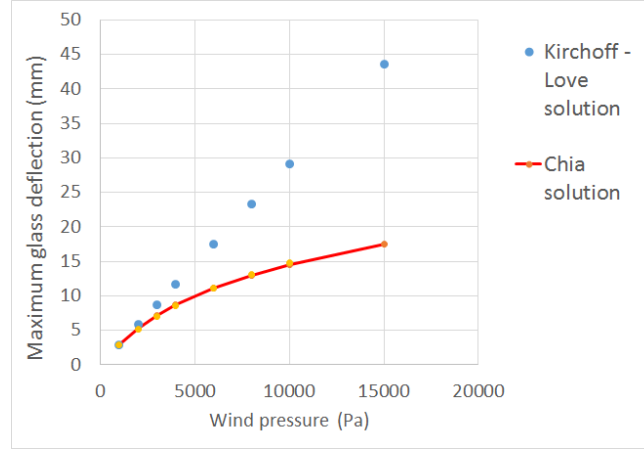


Fig 7: Comparison between the Chia solution (equation 10) of the Von Karman equation of an isotropic plate submitted to a transverse load and the approximated Kirchoff-Love solution (equation 7)

We observe that for a glass deflection of 10mm corresponding to 1% of glass deflection, the deflection calculated by using the KL approximated solution is overestimated by 30% and for a 2% of deflection, it is even overestimated by 60%. For this reason, in a simplified method of joint calculation, the Kirchoff-Love solution should not be used to calculate the angle of rotation α at the edge of the plate because of its narrow domain of validity. Hence, the solution proposed by Chia will be preferred in the current study.

4.2. Integration of the joint effect in the calculation of the angle of rotation at glass edges

In (Descamps 2017), we proposed an equation for the calculation of the maximum joint deformation showing a good agreement with FEA models in a broad range of sealant bite values.

Extending the simplified linear model to the case of a hyperelastic material, we were able to enlarge this domain of validity towards the small bites values for which the joint strain can be over the limit of joint linear elastic behavior.

A small difference between the FEA results and the simplified model remains visible for large bite values (and so large values of the aspect ratio). We associated this difference to the fact that the joint reduces the glass deflection compared to the simply supported assumption and so limits the angle of rotation imposed to the joint. When using the simplified model with the values α calculated by FEA (which takes into account the effect of the joint), a good agreement between the simplified relationship and the FEA modelling was also obtained for very large sealant bites.

Even if the deflection reduction due to the joint is rather limited (10% error on glass deflection at its center for 9mm thick joint with a bite value of 40mm), we propose here below an approximated method to introduce this effect in the simplified joint calculation methodology.

When the glass plate is deflecting, the joint contributes to limit the plate deflection in two ways:

- First, the joint working in shear limits the lateral movement of the edge of the plate, deviating from the simply supported assumption that corresponds to a free lateral movement. As a pure shear is associated to a joint rotation, there is no change in volume and the shear modulus is equal to the material Young's modulus divided by 3 (assuming a Poisson ratio of 0.5 i.e. material incompressibility). This means that the joint contribution in shear does not depend on the joint geometry but only on the bite value. Due to the low material rigidity in shear, we will prove that the contribution of the joint working in shear in the reduction of plate deflection is small.
- Second, the joint working in traction/compression creates a momentum that opposes to the momentum associated to the wind pressure. As in traction/compression the joint rigidity depends on the joint aspect ratio, it will be expected that the reduction of glass deflection associated to the joint working in traction/compression will depend on the joint aspect ratio as well.

Impact of joint reaction force working in shear to limit glass deflection

If external loads are applied in the plane of the plate at both edges, equation 10 becomes (Timoshenko 1987)

$$\frac{D \pi^6}{16 b^4} (1 + \lambda^2)^2 \omega_{1,1} + F_x \omega_{1,1} \frac{\pi^4}{16 a^2 b} + F_y \omega_{1,1} \frac{\pi^4}{16 a b^2} - \frac{E h \pi^6}{8 a^2 b^2} (d_{01} + d_{10}) \omega_{1,1}^3 = q \quad (11)$$

With F_x and F_y , the total reaction forces applied on the x and y edges of the plate.

We observe that the first and the last term of equation (11) are the same than the two terms of equation (10), having the solution of (11) converging to solution of equation (10) when having $F_x=F_y=0$

If we assume a square shaped plate of 1 m^2 surface ($a=b=1, \lambda=1$), the coefficient of the linear term in $\omega_{1,1}$ becomes:

$$\frac{D \pi^6}{4} + F_x \frac{\pi^4}{16} + F_y \frac{\pi^4}{16} \quad (12)$$

If we assume a pane deflection at its center $\omega_{1,1}$ of 1%, we can calculate from equation 9 Δx and Δy , the lateral displacement imposed to the joint associated to plate deflection:

$$\Delta x = \Delta y = \frac{w_{1,1}^2 \pi^2}{8 a} - \frac{3 w_{1,1}^4 \pi^4}{128 a^3} \quad (13)$$

This displacement is very small and equal to $1.23 \cdot 10^{-4}\text{m}$.

Assuming the joint works in shear, we calculate for a square plate, the reaction force of the joint working in shear:

$$F_x = F_y = G \frac{\Delta x}{e_j} W_j a \sim \frac{E \Delta x}{3 x} W_j a \quad (14)$$

G is the sealant shear modulus, E is the sealant Young's modulus, e_j is the joint thickness and W_j , the joint bite.

Assuming a sealant Young's modulus of 1.95MPa Pa , a joint thickness $e_j=6\text{mm}$, a bite $w_j = 20\text{mm}$, we obtain $P_x = P_y \sim 283\text{N}$. Knowing that the flexural rigidity D of a 6mm glass is equal 1400N , we observe that the term associated to glass flexural rigidity (the first term of equation 12) is ~ 2 order of magnitude larger than the contribution associated to the joint. For this reason, we expect a small impact of joint working in shear on the glass plate deflection. We calculate the plate deflection as a function of the sealant bite for the parameters summarized in table 4. The result is shown on figure 8.

Table 4: Parameters used for the calculation of the plate deflection as a function of the sealant bite.

Parameter	Value
Wind pressure	4923 Pa
Small plate dimension a	1.9m
Large plate dimension b	3m
Joint thickness e	9mm
Young modulus- Sealant	1.95E6 Pa
Poisson ratio - Sealant	0.49
Glass thickness h	15.5mm
Young modulus - glass	7E10 Pa
Poisson ratio - Glass	0.3

We observe (figure 8) a very small effect of joint working in shear to limit glass plate deflection, even for sealant bites as large as 40mm.

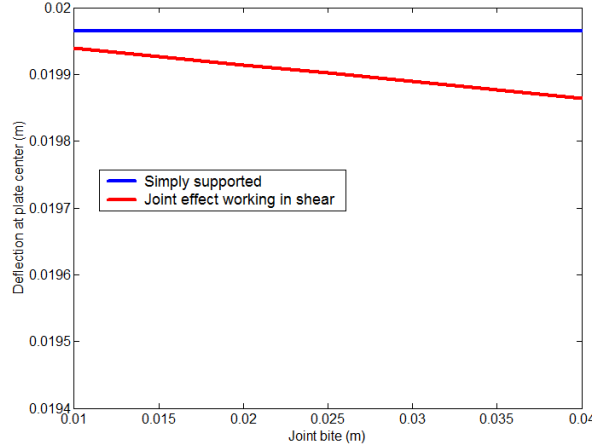


Fig.8:Calculation of the contribution of the joint working in shear on the maximum value of the glass plate deflection at its center change image

Impact of joint reaction force working in tension to limit glass deflection

Working in traction (or partially in traction and in compression depending on the sealant bite value), the joint imposes a momentum to the glass plate and consequently, modifies the amplitude of the deflection of the plate at equilibrium.

The deflection of a plate submitted to an external load can be calculated applying the principle of minimum potential energy. For example, the solution of the Von Karman equation when having simply supported boundary conditions (equation 10) can be obtained applying the minimum potential energy method. The potential energy of a small element (dx, dy) is the sum of the potential strain energy U associated to plate bending (associated to plate spring effect) and the potential energy associated to the external load q (the load multiplied by the displacement associated to plate bending):

$$U(x, y) + q \omega(x, y) dx dy \tag{15}$$

Integrating equation 15 over all plate surface (we use for ω the shape function given by Chia), the total potential energy of the system is obtained. The plate deflection is obtained by minimizing total potential energy, setting to zero the derivative of the total potential energy with respect to ω .

We will now introduce the impact of the joint, applying the minimum potential energy method. Because the plate rigidity is large compared to the joint rigidity in tension, we suppose that the joint will not have a significant impact on the shape function i.e. that the joint will not introduce a local bending close to the plate edges. Hence we assume that the shape function of the plate stays the same. Calculating the potential energy of the system, we have now at the position of the joint:

$$U(x, y) + (q(x, y) - \sigma(x, y)) \omega(x, y) dx dy \tag{16}$$

Where σ is the stress in the joint opposite to external load

Whereas at a plate position different from joint location we have:

$$U(x, y) + q(x, y) \omega(x, y) dx dy \tag{17}$$

Integrating potential energy associated to a small surface element over total plate surface, we obtain the total potential energy:

$$\iint_{S_{plate}} U dx dy + \iint_{S_{plate}-S_{joint}} q(x, y) dx dy + \iint_{S_{joint}} (q(x, y) - \sigma(x, y)) \omega(x, y) dx dy \tag{18}$$

With S_{plate} and S_{joint} , the integration domain corresponding to plate surface and joint surface respectively.

In an equivalent way we can rewrite:

$$tot. pot. energy = \iint_{S_{plate}} U dx dy + \iint_{S_{plate}} q(x, y) dx dy - \iint_{S_{joint}} \sigma(x, y) \omega(x, y) dx dy \quad (19)$$

The last term of equation 19 can be seen as the contribution of the joint working in tension to the total potential energy. Writing the stress σ as a function of joint strain, the term $\iint_{S_{joint}} \sigma(x, y) \omega(x, y) dx dy$ takes the form

$$\iint_{S_{joint}} \frac{E_r}{e_j} (\Delta e + \omega_{1,1} \sin\left(\frac{\pi x}{a}\right) \sin\left(\frac{\pi y}{b}\right)) (\omega_{1,1} \sin\left(\frac{\pi x}{a}\right) \sin\left(\frac{\pi y}{b}\right)) dx dy \quad (20)$$

With E_r = the joint rigidity modulus depending on the joint aspect ratio

The joint strain Δe corresponds to the displacement of the joint working in pure traction, to which is superposed the joint rotation associated to plate bending (Descamps 2017). This quantity is calculated by making the balance of force between the total force associated to the external load q (in our case, homogeneous wind pressure) and the reaction force of the joint

$$\iint_{S_{joint}} \frac{E_r}{e_j} (\Delta e + \omega_0 \sin\left(\frac{\pi x}{a}\right) \sin\left(\frac{\pi y}{b}\right)) dx dy = q a b \quad (21)$$

Equation 19 can now be integrated over plate surface. Then, the plate deformation at the equilibrium is calculated equating to zero the derivation of total potential energy with respect to $\omega_{1,1}$. Carrying-out this calculation, we obtain the following equation:

$$\frac{dU}{d\omega_{1,1}} = \frac{4 a b}{\pi^2} \left(-q + \frac{dW_{joint}}{d\omega_{1,1}} \right) \quad (22)$$

We will note that if we set $q' = -q + \frac{dW_{joint}}{d\omega_{1,1}}$, we retrieve the equation of minimum potential energy of a simply supported plate submitted to an external homogeneous load. Iterating equation 22, starting from solution with no joint contribution, we can calculate the plate deformation using a method simple enough to be implemented in an excel spreadsheet.

The plate deflection at its center calculated using this simplified approach has been compared to the results of a FEA model, using the parameters given in table 4. We observe on figure 9 a relatively good agreement between the glass deflection reduction predicted by the simplified approach and the one calculated by FEA, considering the assumptions made to derive the simplified approach.

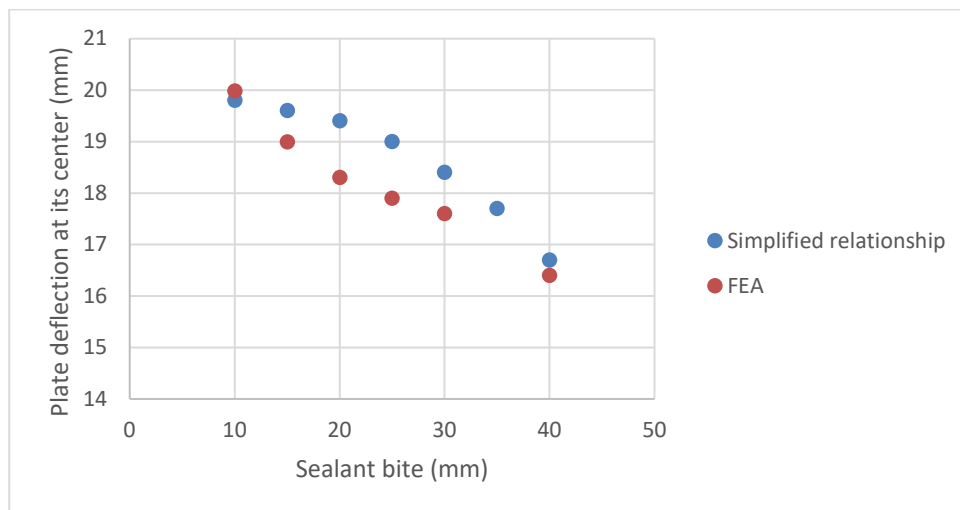


Fig. 9: Comparison between plate deflection at the center using the simplified method including joint effect and the results of FEA modeling.

The glass plate deflection at its center has been combined with the method proposed in (Descamps 2017) to calculate the maximum strain of the joint in the middle of the longer plate side b . These results are compared to the results of 3D FEA simulation (figure 10). First, we observe a sharp decrease followed by a minimum before the joint strain increases again. Making the assumption of a simply supported glass plate to calculate joint rotation overestimates joint strain when having large sealant bites. We observe that both FEA and the simplified method (with the joint limiting

deflection) give very similar results for large bite values: the increase of joint strain for large bites is now reduced, because the joint influences the deformation of the glass plate.

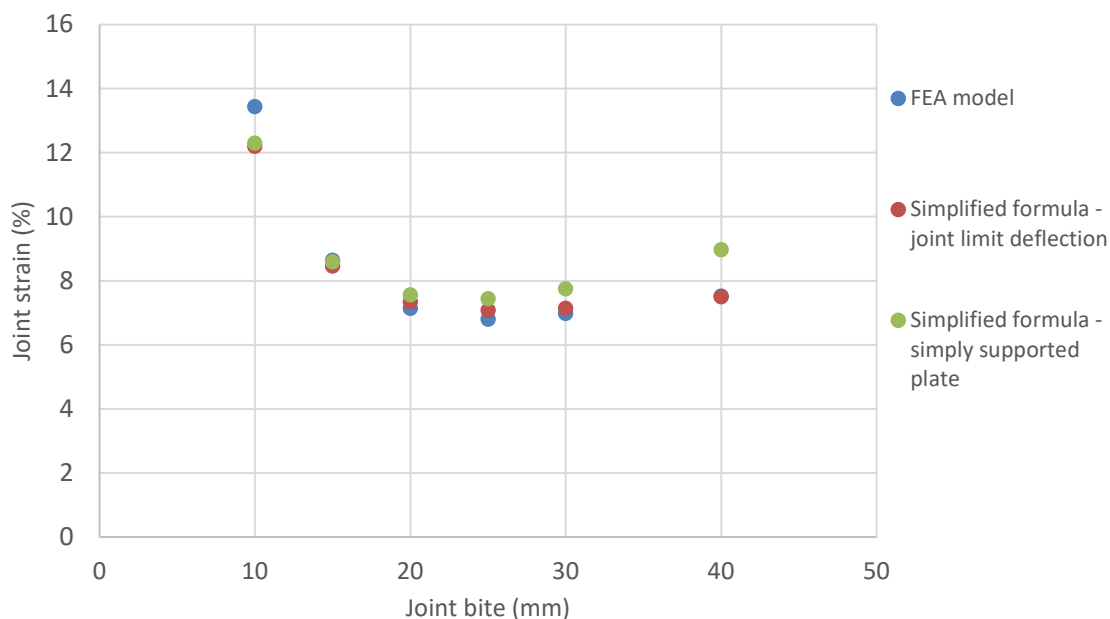


Fig. 10: comparison of maximum value of joint strain as a function of sealant bite for 3D FEA and simplified methods.

5. Conclusion

In this paper, we determined with good accuracy the values of the parameters to be used in the improved equation proposed in (Descamps 2017) as they have a significant impact on the joint deformation and consequently on the conclusions drawn about joint long term durability. The measurement of stress –strain behavior of joint for different geometries confirms that the rigidity factor is only dependent on the joint aspect ratio and not on the absolute joint dimensions. We demonstrated that the joint strain at rupture is also a function of the joint geometry and more precisely of the joint aspect ratio. For this reason, the capability of the joint to accommodate a same deformation increases with decreasing AR. This observation is important as it demonstrates that having a large joint aspect ratio can be detrimental, and that if a large bite value is required to sustain the wind load, the joint thickness must be adjusted accordingly (to decrease joint aspect ratio) to allow the joint to accommodate the maximum deformation imposed by the glass deflection.

The angle of pane bending at its edge is also a critical parameter to be used in this improved equation that includes joint rotation. As a first step in (Descamps 2017), we assumed that the angle of rotation at glass edge could be calculated using a simply supported glass plate assumption. We showed that doing so, the error on joint strain for large bite does not exceed 10%. In this paper, we demonstrated that the plate deflection must be calculated solving the Von Karman equation, since the approximated approach of Kirchhoff-Love (valid for small deflections) leads to significant errors for cases commonly observed in the façade industry. We also proposed a simplified method to calculate plate deflection which takes into account the impact of the joint on the glass plate bending.

This effort is critical to understand the technical recommendations described in the ETAG document, where the use of a most simplified relationship ignoring joint rotation is accepted but only within a very well defined range of application i.e. having a maximum glass maximum deflection below 1% (which limits the plate rotation at its edge) and having a structural joint aspect ratio < 3 which guarantees a minimum flexibility of the joint. For this reason, it is essential when using equations reported in the ETAG document to ensure they are applied within the boundaries specified in the document.

Compared to ETAG equations, this new approach offers additional degrees of freedom to play with in the design of structural joints since the thickness of the joint or the sealant elastic modulus are not part of the ETAG equation. Glass thickness is also a model parameter but this one is partially considered in the ETAG through the limited maximum plate deflection (1%).

Future work will include a final validation of the derived theories by a large scale mockup. This will allow determining the working domain of the improved equations versus the ETAG equations.

References

- ETAG 002, EOTA, Guideline for European technical Approval for Structural Sealant Glazing Kits (SSGK), May 2012
- Descamps et al, *Glass Structures & Engineering* Volume 2 Number 2, 169-182M.: (2017)
- Feynman R. et al., *Lectures on Physics, Vol. II*, 2006, 2010 by California Institute of Technology, Michael A. Gottlieb, and Rudolf Pfeiffer, 1963
- Axel, <http://axelproducts.com/> accessed 20 January 2018
- COMSOL multiphysics, www.comsol.com accessed 20 January 2018
- Chia, C., *Nonlinear Analysis of Plates*, McGraw-Hill 1980
- Chia, C.: Quasimonotonicity, regularity and duality for nonlinear systems of partial differential equations. *Ann. Mat. Pura Appl.* 169, 321–354 (1995)
- Timoshenko S, *Theory of plates and shell*, McGraw-Hill, 1959 (re-ed 1987) ISBN0-07-064779-8